3D Printed Electrochemical Multiwell Plate for Monitoring Food Intolerance from Intestinal Organoids

Emily L. Brooks[1,2], Khalil Hussain[1,2], Khushboo Kotecha[1], Aya Abdalla[1,2], Bhavik Anil Patel[1,2*]

[1]School of Applied Sciences and [2]Centre of Stress and Age-Related Diseases, University of Brighton, Brighton, UK, BN2 4GJ.

* To whom correspondence should be addressed: b.a.patel@brighton.ac.uk

Abstract: Common symptoms of food intolerance are caused by chemical components within food that have a pharmacological activity to alter the motility of the gastrointestinal tract. Food intolerance is difficult to diagnose as it requires a long-term process of eliminating foods that are responsible for gastrointestinal symptoms. Enterochromaffin (EC) cells are key intestinal epithelium cells that respond to luminal chemical stimulants by releasing 5-HT. Changes in 5-HT levels have been shown to directly alter the motility of the intestinal tract. Therefore, a rapid approach for monitoring the impact of chemicals in food components on 5-HT levels can provide a personalised insight into food intolerance and help stratify diets. Within this study we developed a 3D printed electrochemical multiwell plate to determine changes in 5-HT levels from intestinal organoids that were exposed to varying chemical components found in food. The carbon black/poly-lactic acid (CB/PLA) electrodes had a linear range in physiological concentrations of 5-HT (0.1 – 2μM) with a limit of detection of 0.07 μM. The electrodes were stable for monitoring 5-HT overflow from intestinal organoids. Using the electrochemical multiwell plate containing intestinal organoids, increases in 5-HT were observed in the presence of 0.1 mM cinnamaldehyde and 10 mM quercetin but reduction in 5-HT levels was observed in 1 mM sorbitol when compared to control. These changes in the presence of chemicals commonly found in food were verified with *ex vivo* ileum tissue measurements using chromatography and amperometry with boron-doped diamond electrodes. Overall, our 3D electrochemical multiwell plate measurements with intestinal organoids highlight an approach that can be a high-throughput platform technology for rapid screening of food intolerance to provide personalised nutritional diet.

Keywords: 3D printing, enterochromaffin cell, mucosa, serotonin, food intolerance, intestinal organoids

Food intolerance is a nonimmune-mediated adverse reaction to food that can be caused by any non-protein food or food component and is more common than food allergy, which is a reaction of the immune system that mistakenly treats proteins found in food as a threat. Food intolerance can cause symptoms of pain, bloating, trapped wind, constipation and diarrhoea [1,2]. Patients who suffer from irritable bowel syndrome perceive their symptoms are mainly related to food intolerance[3,4]. At present the only way of diagnosing a food intolerance is to monitor symptoms based on the food intake and eliminate those foods which exacerbate your symptoms. However, this can be a long process of trial and error to cut out the suspected food, which can have varying success and drastic impact on the patient diet [5,6].

Symptomatic effects are caused by chemicals present in food with potential pharmacological activity. Not all chemical interactions induce gastrointestinal symptoms, but where they do, the mechanisms are assumed to influence the gastrointestinal neuroendocrine system[3]. Many of the key symptomatic effects occur due to an alteration of intestinal motility. Serotonin (5-HT) which is produced and released by intestinal mucosal enterochromaffin (EC) cells plays a critical role in intestinal motility [7-11]. Release of 5-HT from EC cells activates 5-HT receptors on intrinsic primary afferent neurons. This in turn causes the activation of excitatory and inhibitory motor neurons within the myenteric plexus, which results in contraction and relaxation of intestinal smooth muscle. Therefore, alterations in 5-HT release can have a dramatic effect on motility and can result in varying symptoms such as constipation and diarrhoea. 5-HT can also be associated with nausea and vomiting as it acts on the stomach muscle via vagal pathways [12,13]. Therefore, a high-throughput screening approach which can rapidly monitor changes in 5-HT levels in the presence of chemicals present within food could provide a key stratification process to identify food intolerance.

Electrochemical approaches towards the measurement of 5-HT from EC cells are well established and have provide signficant insight into the role of mucosal 5-HT signalling in physiology and disease [14-22]. Some studies have already highlighted changes in 5-HT levels occur in the presence of odorants, spices and sugars [23-26]. However, these studies have been conducted

on *ex vivo* isolated tissues, which would be challenging to sustain for high throughput studies or more recently on single cells, which lack the complexity of the mucosal epithelium. Intestinal organoids are a three-dimensional *in vitro* model of the intestinal epithelium that allow for robust, specific and high-throughput research of the intestinal epithelium [27-29].

In this study, we developed an electroanalytical approach for the determination of 5-HT from intestinal organoids using a 3D printed electrochemical multiwell plate to identify the impact of different chemicals that are widely present in food and can cause symptoms associated with food intolerance. The chemicals we explored were sorbitol, cinnamaldehyde and quercetin. Sorbitol, a polyol found in many fruits, is of increasing industrial interest as a sweetener, humectant, texturizer and softener[30]. Many studies have shown sorbitol to cause functional gastrointestinal symptoms[31,32]. Cinnamaldehyde provides the odour and taste of the spice cinnamon and has been previously shown to impact 5-HT levels on human intestinal cell models [23,33]. Lastly, quercetin is a flavonoid which is present in many fruits and vegetables, and has been shown to promote gastrointestinal motility [34,35]. Characterisation studies were conducted to investigate the sensitivity and stability of the carbon black/PLA electrodes within the multiwell plate to monitor changes in 5-HT from intestinal organoids.

EXPERIMENTAL METHODS

Fabrication of the 3D printed electrochemical multiwell plate. The 3D printed multiwell plate was designed using SolidWorks (Dassault Systèmes) and a schematic highlighting the key dimensions of the mould as printed is shown in **Figure 1A**. Each well was 20 mm in length and width, with a depth of 13 mm. The 3D printed multiwell plates were printed using PLA on a Raise 3D Pro (Irvine, USA) printer, where the heated bed temperature was 40 °C and the extruder temperature was 210 °C. The multiwell plate was printed with 100 % infill using a printing speed of 3600 mm/s and print layer thickness of 0.1 mm. Two circles and a rounded rectangle are extruded cut into the base of each well to place the electrodes to make an electrochemical cell. All electrodes would be 2 mm in depth, with the working electrode centrally placed with a diameter of 2 mm. The reference electrode was 2.4 mm in diameter and the rounded rectangle was 6 mm in length and was utilised as the counter electrode.

To fabricate the electrodes, the extruded cut circles and rounded rectangle were all filled with carbon black/PLA (marketed as proto pasta, was purchased from filaprint, UK) using a 3D printing pen (SUNLU 300) with a 0.75 mm nozzle and printing speed of 3600 mm/s. When filling the mould, the CB/PLA was compressed whilst in the semi-molten state by mechanical pressure using a metal rod and a coiled silver wire was attached to the semi-molten CB/PLA before being sealed using PLA. To ensure the surface area of the electrode was uniform, the electrodes were mechanically polished using 1200 grit abrasive paper. Following this the surface electrodes were polished in a 0.3 µm alumina suspension for 3 minutes. The reference electrode was then finely painted using silver conductive paint (Electrolube, UK) and placed in chloride bleach based on a previously utilised protocol [36]. A photograph of the final electrochemical multiwell plate can be seen in **Figure 1B**.

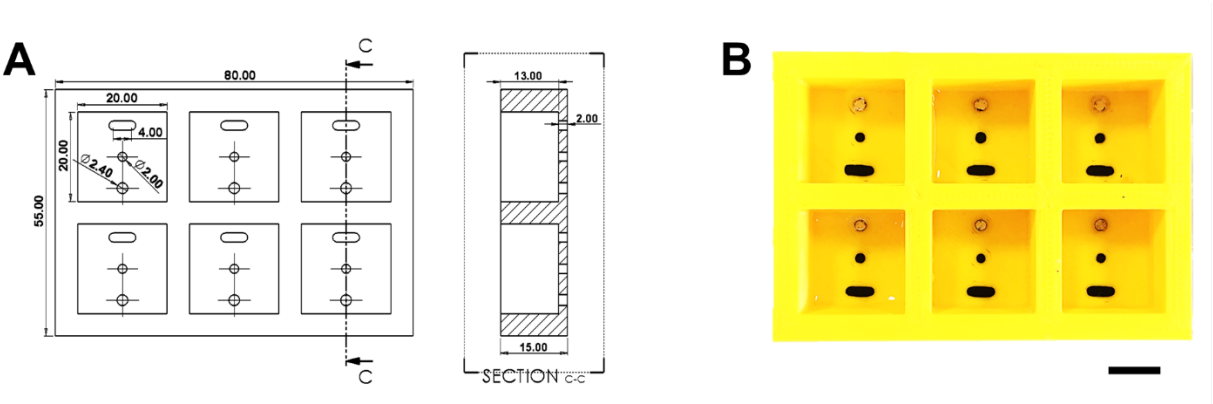

Figure 1. Design of the 3D printed electrochemical multiwell plate. Where (A) displays schematics of the PLA multiwell plate. (B) Photograph of the final 3D printed electrochemical multiwell plate, where the working and auxiliary electrodes were made using CB/PLA and the Ag|AgCl reference electrode was a silver painted CB/PLA electrode which was placed in chloride bleach. The scale bar is 1 cm.

Characterization of 3D electrochemical multiwell plate. Measurements were obtained using CH Instruments 1030B multichannel potentiostat (CH Instruments, Texas, USA). Prior to conducting studies, electrochemical pre-treatment was performed in 0.5 M NaOH by holding the potential at +1.4 V for 200 s and then at -1.0 V for 200 s which has previously been shown to be an effective approach for the activation of CB/PLA electrodes [37,38].

Studies were conducted to investigate the variation in the electrode response within a multiwell plate and between multiwell plates. Cyclic voltammetry studies with 1 mM ferricyanide in 1 M KCl were carried out, where the potential window was -0.3 V to +0.7 V and scan rate of 100 mV/s. To investigate the oxidation peak potential for 5-HT, differential pulse voltammetry (DPV) was utilised, with 10 μM 5-HT in modified Dulbecco's Modified Eagle Medium F12 with 15mM HEPES (DMEM F12). The potential window was 0 to +1 V where the pulse amplitude was 50 mV, the pulse width was 60 mV, sampling period was 0.02 s, and the pulse width was 0.5 s. Calibration responses of 5-HT were conducting using amperometry where the applied voltage was +0.5 V vs Ag|AgCl. Measurements were conducted for a duration of 100 s, where the current response was monitored for 0.1 to 2 μM 5-HT in DMEM F12. For fouling studies, measurements were conducted using solutions of 1 mM ruthenium (III) hexaamine containing 10 μM 5-HT in DMEM F12. Differential pulse voltammograms of 1 mM ruthenium (III) hexaamine were obtained between the voltages of +0.1 to -0.4 V in between amperometric runs in 10 μM 5-HT, where electrodes were held at +0.5 V for a duration of 50 s. This protocol was repeated to record the change in the 1 mM ruthenium (III) hexaamine response after exposure to 5-HT for 300 s. DPVs of 1 mM ruthenium (III) hexaamine were recorded pre-and post-organoid measurements to explore the stability of the electrochemical multiwell plate.

Intestinal organoid preparation. All animal experiments were carried out in compliance with the relevant laws and institution guidelines. Male C57/BL6 mice (6-11 weeks) were euthanized using CO_2 gas then dissected to remove a 10 cm segment of ileum. This was thoroughly washed in cold PBS-Ca-Mg (Gibco) before being cut into 2 mm segments and further washed by pipetting up and down 15-20x in a pre-wetted 10ml serological pipette. Segments were then incubated in gentle cell dissociation reagent (Stemcell technologies) at room temperature for 15 minutes whilst gently rocking. After the incubation, the segments were allowed to settle at the bottom of the tube and the supernatant removed and discarded. Segments were then vigorously resuspended in PBS-Ca-Mg supplemented with 0.1 % BSA (Fisher Scientific) before being allowed to resettle, the supernatant was then passed through a 70 μm cell strainer (Corning) and collected as a crypt fraction. Crypt fraction collection was repeated thrice more, giving crypt fractions 1-4. The Crypt fractions were centrifuged at 290 x *g* for 5 minutes then supernatant discarded. The remaining

pellet was resuspended in 10ml PBS-Ca-Mg 0.1 % BSA, centrifuged at 200 x *g* for 3 minutes then supernatant discarded and resuspended in 10ml cold DMEM F12. The resulting crypt fractions were observed under a microscope and the healthiest fraction was selected for culture. Crypts were counted then the correct volume required was centrifuged at 100 x *g* for 5 minutes then supernatant discarded. The crypts were embedded in a 1:1 ratio of Matrigel (Corning) and Intesticult organoid growth medium (Stemcell technologies) supplemented with 5mg/ml gentamycin and plated at a density of 500 per well in a 24 well plate. Once the Matrigel had set a further 750 µl Intesticult media was added to each well which was changed every 3 days. For passage, the organoid containing Matrigel dome was incubated in 1 ml gentle cell dissociation reagent for 1 minute before being broken up by pipetting and added to a tube containing a further 1 ml gentle cell dissociation reagent and incubated at room temperature for 10 minutes. The organoid mixture was then centrifuged at 290 x *g* for 5 minutes, supernatant discarded, and pellet resuspended in 10ml cold DMEM F12 before being split and re-plated as above. Passage was performed every 7-10 days with a 1:4 split ratio.

Organoid studies using 3D-printed electrochemical multiwell plate. For all experiments organoids were plated at a density of 200 organoids per well in a 1:1 ratio of Matrigel and Intesticult organoid growth medium. This organoid containing hydrogel was directly plated on the working electrode and was covered using 1 ml of DMEM F12.

Initially studies were conducted to explore the change in 5-HT observed in the presence of 1 µM fluoxetine, which we have previously shown to elevate 5-HT overflow in the ileum [14,39,40]. CB/PLA electrodes were run using amperometry where the applied potential was +0.5 V vs Ag|AgCl. Measurements were conducted after 10 and 20 minutes in the presence of 1 µM fluoxetine. Studies were then conducted to explore the impact of different chemicals widely present in food. Organoids were placed in either DMEM F12 or DMEM F12 containing either 1 mM sorbitol, 0.1 mM cinnamaldehyde and 10 mM quercetin for 10 minutes. Measurements were validated using chromatography and amperometry studies using boron-doped diamond (BDD) microelectrodes using *ex vivo* ileum tissue (see ESI for methodology).

Data analysis. For all measurements, the data was plotted to show the mean ± standard deviation. Statistical analysis was carried out using GraphPad Prism, where data was compared using Student t test, one-way ANOVA or two-way ANOVA.

RESULTS AND DISCUSSION

Intra- and inter-variability of electrochemical multiwell plates. Figure 2 shows the intra-variability (differences in the current response between electrodes within a single electrochemical multiwell plate) and inter-variability (differences in the average current response of all the wells between different electrochemical multiwell plates). Initially, measurement was carried out using the inner sphere redox probe ferricyanide. The percentage relative standard deviation (% RSD) was 6.1 % for the ferricyanide cathodic peak current responses when investigating the intra-variability (Figure 2A). The average cyclic voltammogram response for ferricyanide from all six electrodes within a single multiwell plate is shown in Figure 2B for multiple electrochemical multiwell plates. The % RSD for the ferricyanide cathodic peak current increased to 7.6 % for the inter-variability (Figure 2B). These findings highlight excellent precision within and between different electrochemical multiwell plates.

A single oxidation peak for 5-HT was observed at +0.25 ± 0.01 V on the CB/PLA electrodes. Figure 2C shows differential pulse voltammograms of 10 μM 5-HT on different electrodes within a single electrochemical multiwell plate, where the % RSD intra-variability for the 5-HT oxidation peak current was 3.1 %. Figure 2D shows the average response from all electrodes within an electrochemical multiwell plate to compare between different multiple multiwell plates. The % RSD inter-variability for the 5-HT oxidation peak current was 4.5 %. Overall, these findings indicate there is good agreement between individual CB/PLA electrodes within and between electrochemical multiwell plates. Therefore, this 3D printing approach for manufacturing electrochemical multiwell plates provides a suitable way to make uniform devices, which has been shown to be a unique feature of 3D printing[41,42].

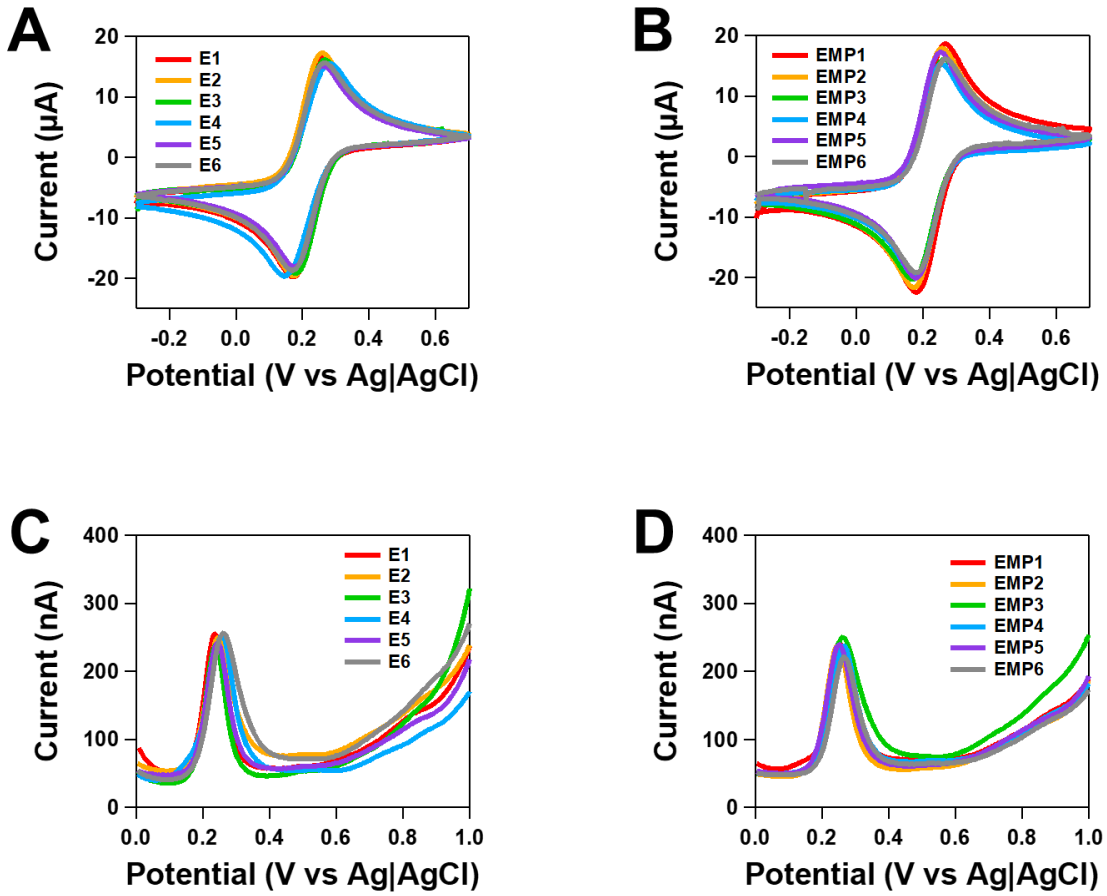

Figure 2. Intra- and inter-variability of the 3D printed electrochemical multiwell plate. Cyclic voltammograms of 1 mM ferrocyanide in 1 M KCl, where (A) shows the intra-variability (differences between electrodes (E) within the six electrode multiwell plate) and (B) shows the inter-variability (comparison of electrochemical multiwell plate (EMP) average responses). Differential pulse voltammograms of 10 µM 5-HT in DMEM F12, where (C) shows the intra-variability and (D) shows the inter-variability.

Investigating the sensitivity and stability of CB/PLA electrodes within the electrochemical multiwell plate. Calibration responses for 5-HT in concentration ranges observed in ileum tissues[7,14] were conducted on electrochemical multiwell plate electrodes. Figure 3A shows amperometry traces obtained for concentrations of 5-HT from 0.1 to 2.0 µM, where responses are shown for electrodes from a single electrochemical multiwell plate. The average responses from the electrodes consisting of six different electrochemical multiwell plates are shown in Figure 3B,

where there was excellent agreement in the calibration responses. Figure 3C shows the overall calibration responses for 5-HT, where the sensitivity was 13.1 nA μM^{-1}. The limit of detection (LOD) was 0.07 μM and the limit of quantification (LOQ) was 0.24 μM. These responses show excellent precision for the detection of 5-HT within physiological ranges observed within ileal mucosa from each individual electrochemical well.

Fouling studies were conducted to explore the stability of the CB/PLA electrodes for measuring 5-HT. For measurements, the reduction peak current of redox probe ruthenium (III) hexaamine was monitored using differential pulse voltammetry following exposure to 10 μM 5-HT every 50 s using amperometry (Figure 3D). Measurements were conducted to monitor the stability of the electrodes after oxidation with 5-HT for 300 s. When comparing the responses of individual electrodes within a single electrochemical multiwell plate (Figure 3E) and the average response from multiple electrochemical multiwell plates (Figure 3F), there was no signficant difference in the reduction peak current when compared to the initial response. These findings highlight that CB/PLA electrodes are stable for the detection of 5-HT over 300 s and not prone to fouling from oxidative by-products of the 5-HT oxidation. This stable response may be due to the nature of the electrode acting as a composite, in which polymeric products due to the by-products of 5-HT oxidation may not have sufficient surface sites to adsorb and reduce the current response of the electrode. Previous studies have also shown CB/PLA electrodes to be stable for electroanalytical monitoring in biological environments[17].

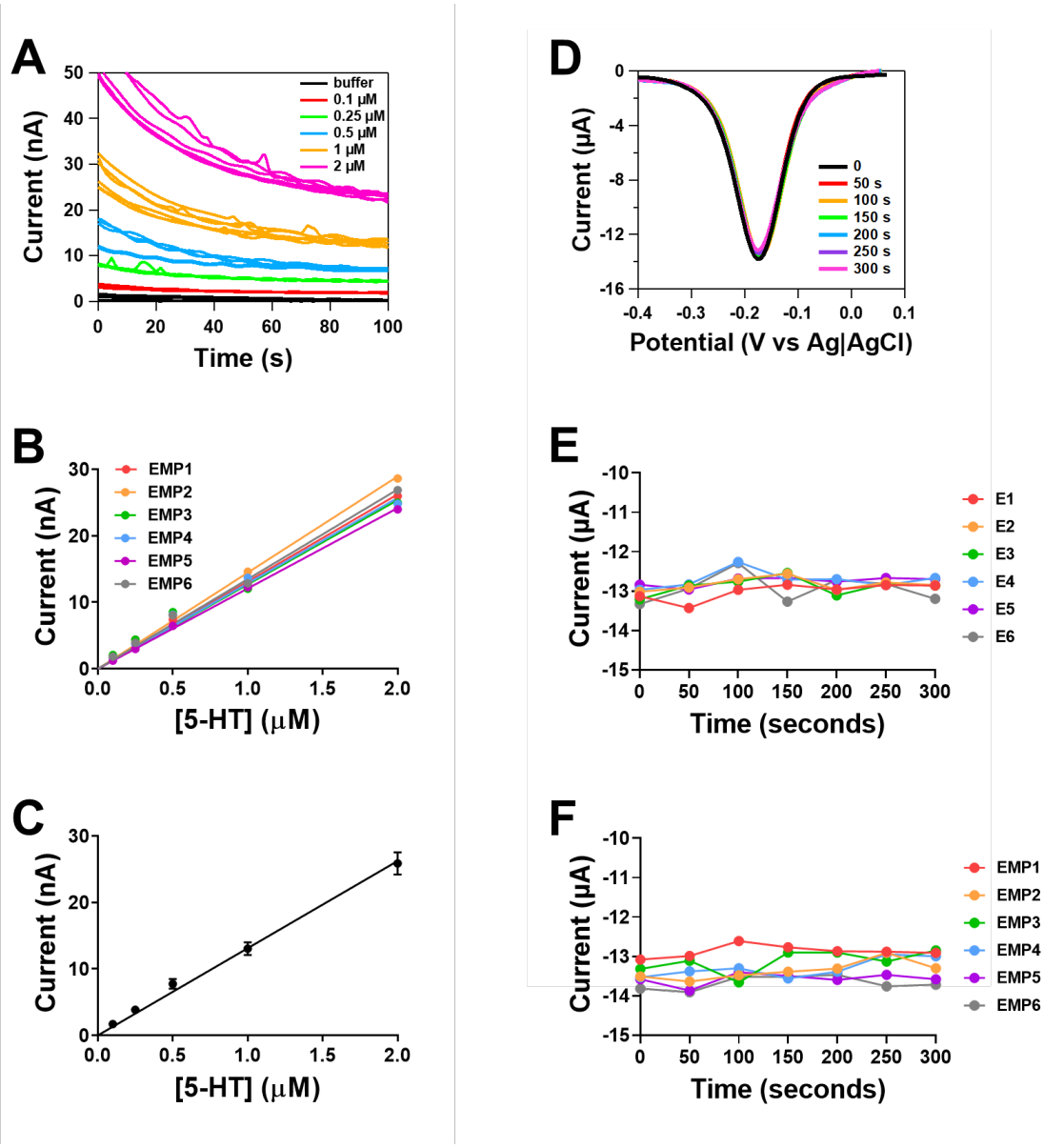

Figure 3. Sensitivity and stability of CB/PLA electrodes. (A) Amperometric responses at +0.5 V for 0.1 to 2 µM 5-HT in DMEM F12. Measurements were recorded for 100 s, where each line at a single concentration represents an individual electrode on a single electrochemical multiwell plate. (B) Linear relationship between concentration and average current response from all CB/PLA electrodes on an electrochemical multiwell plate (EMP), where there was a good agreement between electrochemical multiwell plates. (C) Final calibration for multiple electrochemical multiwell plates, where data is shown as mean ± S.D. and n=6 devices. (D) Differential pulse voltammogram responses of the reduction of ruthenium (III) hexaamine on CB/PLA electrodes which have been exposed to 10 µM 5-HT for varying durations. Responses from (E) all electrodes (E) within a single device and comparison between (F) multiple electrochemical multiwell plates (EMPs).

Growth of organoids and detection of 5-HT using chromatography. Epithelial cells within the intestinal mucosa are constantly replenishing. The epithelium consists of two core domains, the villus and crypts. The crypts within the epithelium contain the intestinal stem cells (ISCs), whilst the villus is composed of several differentiated cell types such as EC cells, which contain 5-HT, and enterocytes which predominantly contain the serotonin transporter (SERT)[27]. By isolating and culturing ISCs over a period of days, the stem cells divide to generate a self-renewing stem cell population, as well as cells that terminally differentiate into enterocytes, enteroendocrine cells or goblet cells (Figure 4A). The terminally differentiated cells are ultimately extruded into the lumen (centre cavity of the organoid) from the villus-like domain, mimicking the physiological turnover of the adult intestinal epithelium (Figure 4B).

Various studies have used biochemical assays to characterise intestinal organoids and verify the presence of EC cells and the machinery present to produce 5-HT[28,29]. Therefore, we utilised chromatography to measure the contents of intestinal organoids to verify if our differentiated ISCs formed EC cells and enterocytes. Figure 4C shows a chromatographic response of approximately 200 intestinal organoids in culture media, mucosa scrapings from 1 cm^2 ileum tissue, the culture media and standards. 5-HT was detected in organoids, suggestive of its production in EC cells. The current response was approximately 5 times greater in the ileum tissue than that observed in intestinal organoids. Additionally, there was a peak that corresponded to 5-HT metabolite 5-hydroxyindoleacetic acid (5-HIAA) in both intestinal organoids and ileum mucosa. 5-HIAA is a metabolite formed from 5-HT following reuptake through SERT and thus is also suggestive of the presence of enterocytes within the organoids. The essential amino acid tryptophan, which is a key synthesis precursor to the production of 5-HT, was also present within ileum mucosa and intestinal organoids. However, for the intestinal organoids, only approximately 30 % of the tryptophan peak observed was present within organoids, as the majority of this response was due to the presence of the chemical in the culture media.

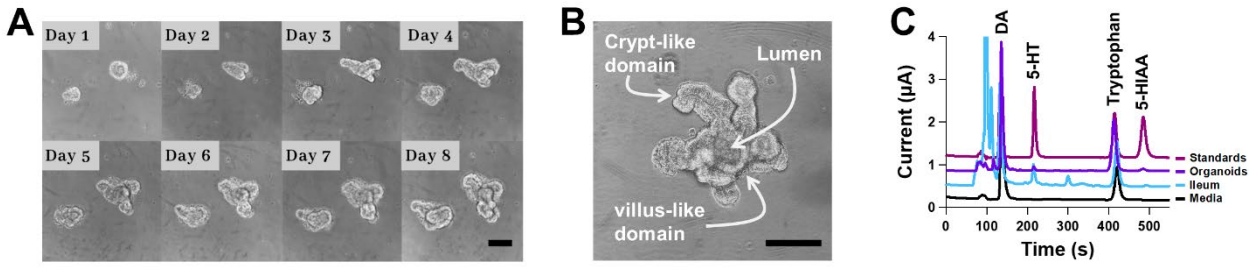

Figure 4. Growth and detection of 5-HT in intestinal organoids. (A) Images showing the eight-day culture of intestinal organoids, where intestinal stem cells (ISCs) differentiate to form intestinal villus epithelium cells. (B) Photograph of a single intestinal organoid, highlighting the lumen, crypt and villus domains. Scale bar is 200 μm. (C) chromatographic measurement of intestinal organoids and mucosal ileum, where presence of 5-HT, 5-HIAA and tryptophan are observed.

Monitoring 5-HT overflow from intestinal organoids. The chromatographic studies clearly showed the presence of 5-HT within intestinal organoids and thus we investigated if the overflow of 5-HT from intestinal organoids could be determined on CB/PLA electrodes within the electrochemical multiwell plate. Figure 5A shows a differential pulse voltammogram taken from intestinal organoids where two oxidation peaks were observed. The first oxidation peak observed at +0.22 V corresponds to the presence of 5-HT as verified by a standard. Compared to the 5-HT standard, the peak response of 5-HT is much broader, which is most likely due to the slower diffusion through the hydrogel layer in which the organoids are present. The second oxidation peak was at + 0.66 V, and corresponds to melatonin, which has been previously identified when conducting measurements from mucosal ileum tissue[40]. These findings indicate that selective detection of 5-HT can be achieved by applying +0.5 V.

To further verify that 5-HT was detected on the CB/PLA electrodes, measurements were conducted using SERT blocker fluoxetine. These studies would also indicate if SERT protein was expressed by the enterocytes within the intestinal organoids. Figure 5B shows the response from a single electrochemical multiwell plate where three wells were monitoring 5-HT overflow in DMEM F12 and other three wells were monitoring 5-HT overflow in DMEM F12 containing 1 μM fluoxetine. These measurements also provide the ability to explore the variability between wells which were all loaded with approximately 200 organoids. By comparing the 5-HT oxidation current from 18 wells that contained intestinal organoids, the RSD was 22 %. Although this is a

high deviation, this was expected due to variations in loading amount of healthy intestinal organoids. Figure 5B shows that there was an increase in the current due to the oxidation of 5-HT after 10 and 20 mins in wells that contained 1 μM fluoxetine. The overall responses are shown in Figure 5C, where there was a signficant increase in the concentration of 5-HT after 10 and 20 mins ($p<0.001$, $n=6$) in the presence of 1 μM fluoxetine. This increase is due to blocking of SERT, thus increasing extracellular levels of 5-HT. Overall these studies highlight that intestinal organoids provide a unique and high-throughput model system for understanding the impact of therapeutic drugs and chemical agents on the overflow of 5-HT.

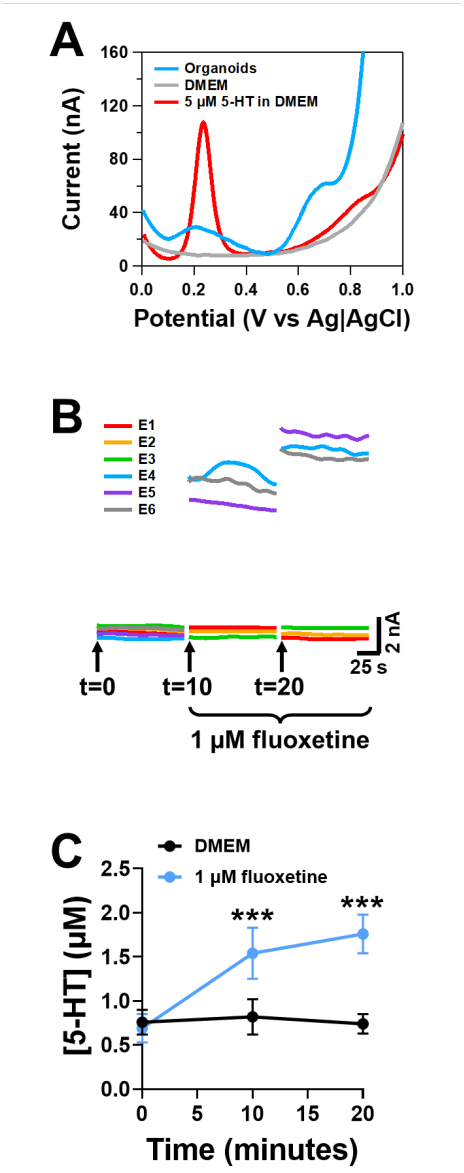

Figure 5. Detection of 5-HT overflow from intestinal organoids. (A) Differential pulse voltammograms obtained from intestinal organoids and the background hydrogel / DMEM F12. The response of 5 µM 5-HT is shown for comparison. (B) Amperometry responses of intestinal organoids at +0.5 V vs Ag|AgCl reference electrode, where three wells contained DMEM F12 and three contained 1 µM fluoxetine in DMEM F12. (C) Change in 5-HT concentration from intestinal organoids in the presence of 1 µM fluoxetine, where data is shown as mean ± S.D., n=6 and ***p<0.001.

Understanding the impact of chemicals widely found in food on 5-HT overflow. Studies were conducted to understand the impact of different chemicals which are widely present in food on the overflow of 5-HT from intestinal organoids. Changes in 5-HT levels can have a profound impact on bowel motility and can lead to symptoms of constipation and diarrhoea, which are often an unpleasant effect of food intolerance. Using the multiwell plate, figure 6A shows amperometric response obtained from intestinal organoids in DMEM F12 containing either 1 mM sorbitol, 0.1 mM cinnamaldehyde, 10 mM quercetin and 1 mM glucose. These concentrations were chosen based on previously published studies. Response to the chemicals were compared to the control response obtained from intestinal organoids in DMEM F12. Figure 6B shows that 5-HT levels were reduced in 1 mM sorbitol but elevated in 0.1 mM cinnamaldehyde and 10 mM quercetin when compared to DMEM F12 ($p<0.001$, $n=6$). There was a greater increase in 5-HT level in 10 mM quercetin when compared to 0.1 mM cinnamaldehyde. No differences in 5-HT were observed in 1 mM glucose. The changes in 5-HT observed with intestinal organoids support studies which have been conducted in *ex vivo* ileum tissues and BON cells[23,24]. These findings can provide important insight into the functional changes within the bowel as reductions in 5-HT, as observed in the presence of sorbitol, will reduce motility and thus lead to constipation. Minor increases in 5-HT have been shown to be pro-kinetic and thus increase motility, which would be expected in the case of cinnamaldehyde and thus may lead to diarrhoea. However, even greater increases in 5-HT, akin to those observed in the presence of SERT inhibitors can desensitize 5-HT receptors and reduce motility[17,43]. This may occur in the presence of quercetin, which would potentially lead to constipation.

To verify these changes, measurements were conducted in ileal mucosal scrapings using liquid chromatography and *ex vivo* ileum tissue using amperometry, which have been widely used approaches for monitoring 5-HT overflow from the intestinal tract[22,44-47]. Figure 6C shows chromatographic traces in which the inset highlights the amplitude of the peak corresponding to 5-HT. The overall response is shown in Figure 6D, where there is a signficant decrease in 5-HT levels from ileum tissue in the presence of 1 mM sorbitol but significant increase in 5-HT levels in the presence of in 0.1 mM cinnamaldehyde and 10 mM quercetin when compared to DMEM F12 ($p<0.001$, $n=6$). No differences in 5-HT were observed in 1 mM glucose. Amperometric traces were obtained using a BDD microelectrode over an ex vivo ileum segment (Figure 6E), where clear differences in the amplitude of the current were observed in the presence of the various

chemical agents. Figure 6F shows that 5-HT levels were reduced in 1 mM sorbitol but elevated in 0.1 mM cinnamaldehyde and 10 mM quercetin when compared to DMEM F12 ($p<0.001$, $n=6$). No differences in 5-HT were observed in 1 mM glucose.

The results obtained from amperometric measurement from tissue segments and chromatography measurement from mucosal scapings yielded the same trends as those observed in intestinal organoid measurements. However, the scale of these changes was slightly different, with a greater elevation in 5-HT observed in the presence of quercetin when compared to DMEM F12 from studies conducted on *ex vivo* ileum when compared to intestinal organoids. This may be due to the lack of innervation from the myenteric plexus which would not be present within intestinal organoids. These findings suggest that organoids can provide a useful and effective biological model of the intestinal epithelium for exploring serotonergic signalling from EC cells. Studies with organoids provide the means to reduce the number of animals used but also can replace the use animals by using human organoid models. Additionally, intestinal organoids provide a useful means of conducting high-throughput studies, which would make it a reality to screen multiple chemicals widely present in food. Such developments can provide personalised nutrition management for people suffering with food intolerance.

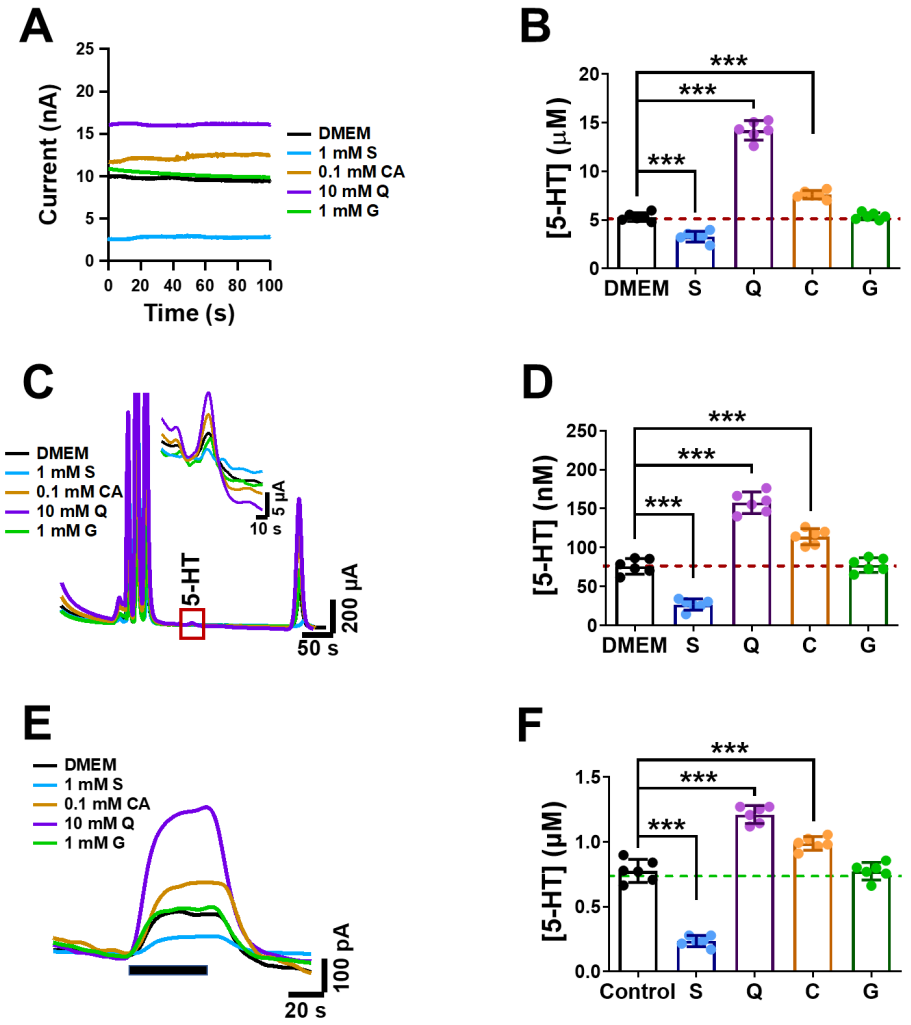

Figure 6. Impact of chemicals present in food on 5-HT levels. Studies were conducted using DMEM F12 containing either 1 mM sorbitol (S), 0.1 mM cinnamaldehyde (CA), 10 mM quercetin (Q) and 1 mM glucose (G). Measurements conducted using intestinal organoids, where (A) shows amperometric traces at +0.5 V vs Ag|AgCl and (B) shows overall responses. Measurements were conducted using mucosal scapings from *ex vivo* ileum tissue using liquid chromatograph, where (C) shows chromatographs with inset highlighting the 5-HT peak (red box). The overall responses are shown in (D). Measurements conducted on ex vivo ileum tissue using amperometry with BDD microelectrodes. The electrode was held at +0.65 V vs Ag|AgCl, where (E) shows amperometric traces and the bar indicates the duration in which the electrode was held 100 µm over the tissue. The overall responses are shown in (F). All data is shown as mean ± S.D., where n=6 and ***p<0.001.

Stability of electrodes for monitoring 5-HT overflow from organoids. The stability of the CB/PLA electrodes were investigated following measurements in intestinal organoids. Differential pulse voltammograms of 1 mM ruthenium hexaamine were obtained before and after measurement intestinal organoids (Figure 7A). There was no difference between the current response obtained after measurements with intestinal organoids when compared to the initial response (n = 6, Figure 7B). These findings indicate that the CB/PLA electrodes are stable for the duration of measurements with intestinal organoids. We had already shown that the electrodes were not prone to fouling from 5-HT oxidative by-products (Figure 3), but these findings indicate that electrodes were not affected by biofouling from the intestinal organoids. This is due to the influence of the Matrigel layer in which organoids are present also acting as a barrier to protect the electrode and sustain the lifespan of the electrode for measurements.

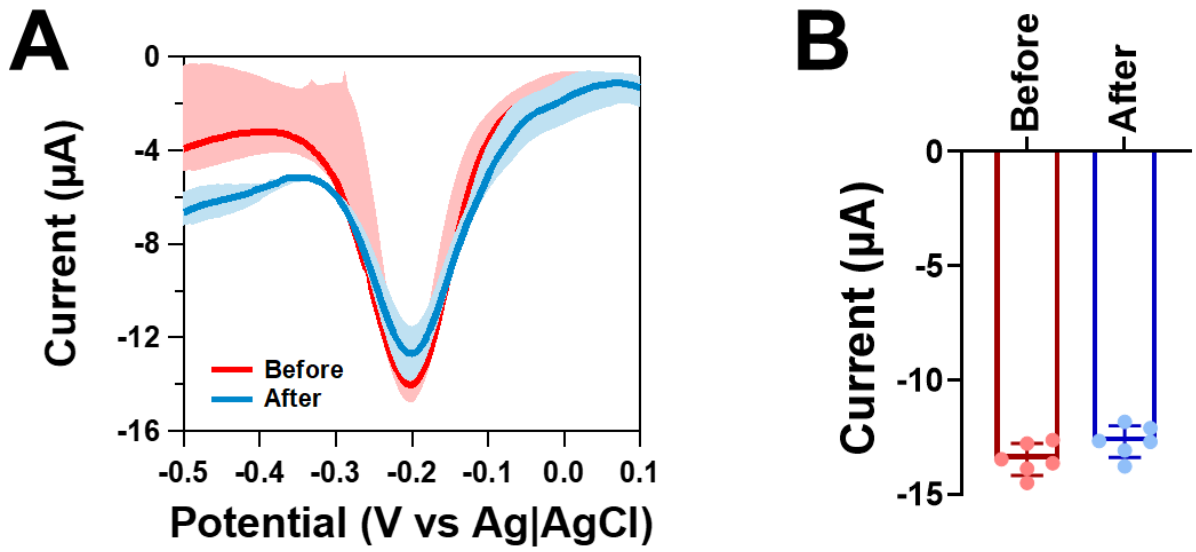

Figure 7. Stability of CB/PLA electrodes following measurements in intestinal organoids. (A) shows differential pulse voltammograms of ruthenium hexaamine before and after measurements in intestinal organoids, where the solid line indicates the mean response and shaded area highlights the standard deviation. (B) shows the overall current response before and after intestinal organoid measurements, where no difference was observed.

CONCULSIONS

We developed a 3D printed multiwell plate that contained CB/PLA electrodes, which was able to detect physiological concentrations of 5-HT without any significant electrode fouling from intestinal organoids. The electrochemical multiwell plate was able to clearly detect changes in 5-HT overflow from intestinal organoids that were exposed to chemicals which are widely found in food and are known to alter intestinal motility. These findings were verified using chromatography and amperometry employing BDD electrodes from ex vivo intestinal tissue. Overall, our electrochemical multiwell plates provide the means to rapidly monitor changes in 5-HT which can be conducted in a high-throughput manner allowing for the ability to screen a host of chemicals to understand which can cause the symptoms of food intolerance. Such understanding will provide key personalised insight into diet management to support wellbeing.

Supporting Information

Experimental details on chromatography experiments and amperometric studies conducted using boron doped diamond electrodes (DOC)

AUTHOR INFORMATION

Corresponding author: Bhavik Anil Patel – School of Applied Science, Centre for Stress and Age-Related Disease, University of Brighton, Moulsecoomb Campus, Brighton, East Sussex, BN2 4GJ; UK; orcid.org/0000-0002-8773-3850; Email: b.a.patel@brighton.ac.uk

ORCID

Emily L. Brooks: 0000-0003-3561-8399

Khalil K. Hussain: 0000-0003-0861-3314

Aya Abdalla: 0000-0001-7814-1442

Bhavik Anil Patel: 0000-0002-8773-3850

Author Credit

The manuscript was written through contributions of all authors. All authors have given approval to the final version of the manuscript. EB, KH, KK, AA and BAP conducted the experiments, data analysis, and contributed to the writing of the manuscript. Intestinal organoids were prepared by EB. The 3D printed electrochemical multiwell plates were prepared by EB, KH and AA. HPLC studies were conducted by KK and EB. KH conducted electrochemical characterisation studies. Organoid studies were conducted by EB and BAP. BAP contributed to the design of the experiments, review of the experimental results, and writing of the manuscript.

Notes

The authors declare no competing financial interest.

REFERENCES

(1) Farah, D.; Calder, I.; Benson, L.; MacKenzie, J. Specific food intolerance: its place as a cause of gastrointestinal symptoms, *Gut* **1985**, *26*, 164-168.

(2) Gibson, P. R. Food intolerance in functional bowel disorders, *Journal of gastroenterology and hepatology* **2011**, *26*, 128-131.

(3) Lomer, M. The aetiology, diagnosis, mechanisms and clinical evidence for food intolerance, *Alimentary pharmacology & therapeutics* **2015**, *41*, 262-275.

(4) Hayes, P. A.; Fraher, M. H.; Quigley, E. M. Irritable bowel syndrome: the role of food in pathogenesis and management, *Gastroenterology & hepatology* **2014**, *10*, 164.

(5) McKenzie, Y.; Alder, A.; Anderson, W.; Wills, A.; Goddard, L.; Gulia, P.; Jankovich, E.; Mutch, P.; Reeves, L.; Singer, A. British Dietetic Association evidence-based guidelines for the dietary management of irritable bowel syndrome in adults, *Journal of Human Nutrition and Dietetics* **2012**, *25*, 260-274.

(6) Staudacher, H. M.; Irving, P. M.; Lomer, M. C.; Whelan, K. Mechanisms and efficacy of dietary FODMAP restriction in IBS, *Nature reviews Gastroenterology & hepatology* **2014**, *11*, 256-266.

(7) Bertrand, P. P. Real-time measurement of serotonin release and motility in guinea pig ileum, *J Physiol* **2006**, *577*, 689-704.

(8) Galligan, J. J.; Parkman, H. Recent advances in understanding the role of serotonin in gastrointestinal motility and functional bowel disorders, *Neurogastroenterology & Motility* **2007**, *19*, 1-4.

(9) Gershon, M. D. Serotonin Receptors and Transporters - Roles in Normal and Abnormal Gastrointestinal Motility, *Alimentary Pharmacology and Therapeutics* **2004**, *20*, 3 -14.
(10) Morris, R.; Fagan-Murphy, A.; MacEachern, S. J.; Covill, D.; Patel, B. A. Electrochemical fecal pellet sensor for simultaneous real-time ex vivo detection of colonic serotonin signalling and motility, *Scientific Reports* **2016**, *6*, 23442.
(11) Patel, B. A. Mucosal serotonin overflow is associated with colonic stretch rather than phasic contractions, *Neurogastroenterology & Motility* **2016**, *28*, 914-923.
(12) Babic, T.; Browning, K. N. The role of vagal neurocircuits in the regulation of nausea and vomiting, *European journal of pharmacology* **2014**, *722*, 38-47.
(13) Browning, K. N. Role of central vagal 5-HT3 receptors in gastrointestinal physiology and pathophysiology, *Frontiers in Neuroscience* **2015**, *9*, 413.
(14) Marcelli, G.; Patel, B. A. Understanding changes in uptake and release of serotonin from gastrointestinal tissue using a novel electroanalytical approach, *Analyst* **2010**, *135*, 2340-2347.
(15) Raghupathi, R.; Duffield, M. D.; Zelkas, L.; Meedeniya, A.; Brookes, S. J. H.; Sia, T. C.; Wattchow, D. A.; Spencer, N. J.; Keating, D. J. Identification of unique release kinetics of serotonin from guinea-pig and human enterochromaffin cells, *The Journal of Physiology* **2013**, *591*, 5959-5975.
(16) Samuel Tran, V.; Marion-Audibert, A. M.; Karatekin, E.; Huet, S.; Cribier, S.; Guillaumie, K.; Chapuis, C.; Desnos, C.; Darchen, F.; Henry, J. P. Serotonin Secretion by Human Carcinoid BON Cells, *Annals of the New York Academy of Sciences* **2004**, *1014*, 179-188.
(17) Hamzah, H. H.; Keattch, O.; Yeoman, M. S.; Covill, D.; Patel, B. A. Three-Dimensional-Printed Electrochemical Sensor for Simultaneous Dual Monitoring of Serotonin Overflow and Circular Muscle Contraction, *Analytical Chemistry* **2019**, *91*, 12014-12020.
(18) MacEachern, S. J.; Keenan, C. M.; Papakonstantinou, E.; Sharkey, K. A.; Patel, B. A. Alterations in melatonin and 5-HT signalling in the colonic mucosa of mice with dextran-sodium sulfate-induced colitis, *British Journal of Pharmacology* **2018**, *175*, 1535-1547.
(19) Patel, B. A. Electroanalytical approaches to study signaling mechanisms in the gastrointestinal tract, *Neurogastroenterology & Motility* **2011**, *23*, 595-605.
(20) Patel, N.; Fagan-Murphy, A.; Covill, D.; Patel, B. A. 3D Printed Molds Encompassing Carbon Composite Electrodes To Conduct Multisite Monitoring in the Entire Colon, *Analytical Chemistry* **2017**, *89*, 11690-11696.
(21) Bertrand, P. P.; Barajas-Espinosa, A.; Neshat, S.; Bertrand, R. L.; Lomax, A. E. Analysis of real-time serotonin (5-HT) availability during experimental colitis in mouse, *Am J Physiol Gastrointest Liver Physiol* **2010**, *298*, G446-455.

(22) Patel, B. A.; Bian, X.; Quaiserova-Mocko, V.; Galligan, J. J.; Swain, G. M. *In vitro* continuous amperometric monitoring of 5-hydroxytryptamine release from enterochromaffin cells of the guinea pig ileum, *The Analyst* **2007**, *132*, 41-47.
(23) Braun, T.; Voland, P.; Kunz, L.; Prinz, C.; Gratzl, M. Enterochromaffin cells of the human gut: sensors for spices and odorants, *Gastroenterology* **2007**, *132*, 1890-1901.
(24) Kim, M.; Cooke, H. J.; Javed, N. H.; Carey, H. V.; Christofi, F.; Raybould, H. E. d-Glucose releases 5-hydroxytryptamine from human bon cells as a model of enterochromaffin cells, *Gastroenterology* **2001**, *121*, 1400-1406.
(25) Raybould, H. E. Does Your Gut Taste? Sensory Transduction in the Gastrointestinal Tract, *Physiology* **1998**, *13*, 275-280.
(26) Wang, Y.; Sims, C. E.; Allbritton, N. L. Enterochromaffin cell-enriched monolayer platform for assaying serotonin release from human primary intestinal cells, *Analytical chemistry* **2020**, *92*, 12330-12337.
(27) Taelman, J.; Diaz, M.; Guiu, J. Human Intestinal Organoids: Promise and Challenge, *Frontiers in Cell and Developmental Biology* **2022**, *10*.
(28) Tsuruta, T.; Saito, S.; Osaki, Y.; Hamada, A.; Aoki-Yoshida, A.; Sonoyama, K. Organoids as an ex vivo model for studying the serotonin system in the murine small intestine and colon epithelium, *Biochemical and Biophysical Research Communications* **2016**, *474*, 161-167.
(29) Zachos, N. C.; Kovbasnjuk, O.; Foulke-Abel, J.; In, J.; Blutt, S. E.; De Jonge, H. R.; Estes, M. K.; Donowitz, M. Human enteroids/colonoids and intestinal organoids functionally recapitulate normal intestinal physiology and pathophysiology, *Journal of Biological Chemistry* **2016**, *291*, 3759-3766.
(30) Silveira, M.; Jonas, R. The biotechnological production of sorbitol, *Applied microbiology and biotechnology* **2002**, *59*, 400-408.
(31) Hyams, J. S. Sorbitol intolerance: an unappreciated cause of functional gastrointestinal complaints, *Gastroenterology* **1983**, *84*, 30-33.
(32) Jain, N.; Rosenberg, D.; Ulahannan, M.; Glasser, M.; Pitchumoni, C. Sorbitol intolerance in adults, *American Journal of Gastroenterology (Springer Nature)* **1985**, *80*.
(33) Doihara, H.; Nozawa, K.; Kojima, R.; Kawabata-Shoda, E.; Yokoyama, T.; Ito, H. QGP-1 cells release 5-HT via TRPA1 activation; a model of human enterochromaffin cells, *Molecular and Cellular Biochemistry* **2009**, *331*, 239-245.
(34) Liu, W.; Zhi, A. The potential of Quercetin to protect against loperamide-induced constipation in rats, *Food Science & Nutrition* **2021**, *9*, 3297-3307.
(35) Kim, J. E.; Lee, M. R.; Park, J. J.; Choi, J. Y.; Song, B. R.; Son, H. J.; Choi, Y. W.; Kim, K. M.; Hong, J. T.; Hwang, D. Y. Quercetin promotes gastrointestinal motility and mucin secretion in loperamide-

induced constipation of SD rats through regulation of the mAChRs downstream signal, *Pharmaceutical biology* **2018**, *56*, 309-317.

(36) Rohaizad, N.; Mayorga-Martinez, C. C.; Novotný, F.; Webster, R. D.; Pumera, M. 3D-printed Ag/AgCl pseudo-reference electrodes, *Electrochemistry Communications* **2019**, *103*, 104-108.

(37) Richter, E. M.; Rocha, D. P.; Cardoso, R. M.; Keefe, E. M.; Foster, C. W.; Munoz, R. A. A.; Banks, C. E. Complete Additively Manufactured (3D-Printed) Electrochemical Sensing Platform, *Analytical Chemistry* **2019**, *91*, 12844-12851.

(38) Rocha, D. P.; Squissato, A. L.; da Silva, S. M.; Richter, E. M.; Munoz, R. A. A. Improved electrochemical detection of metals in biological samples using 3D-printed electrode: Chemical/electrochemical treatment exposes carbon-black conductive sites, *Electrochimica Acta* **2020**, *335*, 135688.

(39) Bertrand, P. P.; Hu, X.; Mach, J.; Bertrand, R. L. Serotonin (5-HT) release and uptake measured by real-time electrochemical techniques in the rat ileum, *Am J Physiol Gastrointest Liver Physiol* **2008**, *295*, G1228-1236.

(40) Patel, B. A. Continuous amperometric detection of co-released serotonin and melatonin from the mucosa in the ileum., *The Analyst* **2008**, *133*, 516-524.

(41) Singh Shergill, R.; Perez, F.; Abdalla, A.; Anil Patel, B. Comparing electrochemical pre-treated 3D printed native and mechanically polished electrode surfaces for analytical sensing, *Journal of Electroanalytical Chemistry* **2022**, *905*, 115994.

(42) O'Neil, G. D.; Ahmed, S.; Halloran, K.; Janusz, J. N.; Rodríguez, A.; Terrero Rodríguez, I. M. Single-step fabrication of electrochemical flow cells utilizing multi-material 3D printing, *Electrochemistry Communications* **2019**, *99*, 56-60.

(43) Lavoie, B.; Tchitchkan, D.; Mawe, G. Abundant 5-HT Release from EC Cells Disrupts Colonic Motility, *The FASEB Journal* **2015**, *29*, 1002.1010.

(44) Brooks, E. L.; Mutengwa, V. S.; Abdalla, A.; Yeoman, M. S.; Patel, B. A. Determination of tryptophan metabolism from biological tissues and fluids using high performance liquid chromatography with simultaneous dual electrochemical detection, *Analyst* **2019**, *144*, 6011-6018.

(45) Bian, X.; Patel, B.; Dai, X.; Galligan, J. J.; Swain, G. High Mucosal Serotonin Availability in Neonatal Guinea Pig Ileum Is Associated With Low Serotonin Transporter Expression, *Gastroenterology* **2007**, *132*, 2438-2447.

(46) Lwin, A.; Patel, B. A. High performance liquid chromatography method for the detection of released purinergic and biogenic amine signaling molecules from in vitro ileum tissue, *Journal of Separation Science* **2010**, *33*, 1538-1545.

(47) Bertrand, P. P. Real-time detection of serotonin release from enterochromaffin cells of the guinea-pig ileum, *Neurogastroenterology and motility : the official journal of the European Gastrointestinal Motility Society* **2004**, *16*, 511-514.

TOC